

On Algorithms for Planning S-curve Motion Profiles

Kim Doang Nguyen; Teck-Chew Ng and I-Ming Chen

Robotics Research Center, Nanyang Technological University, Singapore

Corresponding author E-mail: z030004@ntu.edu.sg

Abstract: Although numerous researches on s-curve motion profiles have been carried out, up to date, no systematic investigation on the general model of polynomial s-curve motion profiles is considered. In this paper, the model of polynomial s-curve motion profiles is generalized in a recursive form. Based on that, a general algorithm to design s-curve trajectory with time-optimal consideration is proposed. In addition, a special strategy for planning s-curve motion profiles using a trigonometric model is also presented. The algorithms are implemented on a linear motor system. Experimental results show the effectiveness and promising application ability of the algorithms in s-curve motion profiling.

Keywords: Motion control, s-curve motion profile, trajectory planning algorithm, linear motor.

1. Introduction

Control theory is now understood not merely in the narrow sense of the control of mechanisms but in wider sense of the control of any dynamic system, for example economics, finance, industrial processes, etc, and even nature. As a key aspect of control theory, motion control has a wide range of applications in industry, such as manufacturing, targeting, robotics, etc. In motion control systems, controllers are used together with closed loops to control the velocity and position of machines in order to generate desired motions. The challenge in motion control is always how to achieve precise motion with minimized vibration, and overshoot in position as well as velocity. In the attempt to solve the challenge, trajectory planning has been extensively researched for a few decades. Mechanically feasible and smooth paths with optimized time and minimized overshoots are always the goals of path planning.

It is well accepted that simple trapezoidal velocity models, in which the motor is accelerated to a constant velocity at a constant acceleration and decelerated to zero at a constant deceleration, can achieve fast motions. However as shown in Fig.1 (a), when the velocity reach the maximum value at the time instant t_1 , the acceleration jumps from its constant value to zero. The jumps also occur at other time instants, t_0 , t_2 , t_3 when the velocity changes its orientation. These discontinuities of the acceleration make the jerk exhibit infinite values. Therefore trapezoidal velocity profiles tend to cause overshoots, and excite residual vibrations that require time for the machine to reach the final position with desired precision (Lin, 2002). This may be a potential problem for precision system. As a result, s-

curve velocity profiles have been proposed to reduce the tendency to excite system vibration (Roover, 1997), (Levin, 1994) and (Meckl, 1985). In these s-curve models the template is kept in controllable finite value.

In (Meckl, 1998), a method for developing optimized point-to-point motion profile to attain fast motion with minimized vibration is proposed using s-curve model. The research gave a guide to estimate the ramp-up and ramp-down time. In the attempt of improving the kinematic and dynamic performance of a punching machine, Tsay and Lin developed an input strategy with fast acceleration and slow deceleration to minimize the residual response based on 3rd order polynomial s-curve motion profiles (Tsay, 2005). In addition a time-optimal solution in feedback form was discussed through state-space analysis of a single DOF closed-loop system whose actuator is a linear brushless DC motor (Kim, 2003). The research also provided a categorization of 3rd order polynomial s-curve models. Macfarlane and Croft, (Macfarlane, 2003), developed an online method for attaining smooth, jerk-bounded trajectories, which was described as no oscillation and near time optimal paths. In the method a sine-wave template is used to compute control way-points, which are then connected smoothly by 5th order polynomials. This model can be considered as a combination of a 5th order polynomial model and a trigonometric model.

Although various researches on s-curve motion profiles have been carried out, up to date, no systematic investigation on the general model of polynomial s-curve motion profiles is considered. In this paper, the generalization of the polynomial s-curve model was presented together with the proposal of a general algorithm to design s-curve motion trajectory. Moreover the research on a trigonometric model, which

is a combination of trigonometric and polynomial functions, indicates a special strategy of path planning for s-curve motions. Through experimental results, the algorithms show their efficiency, and great application ability.

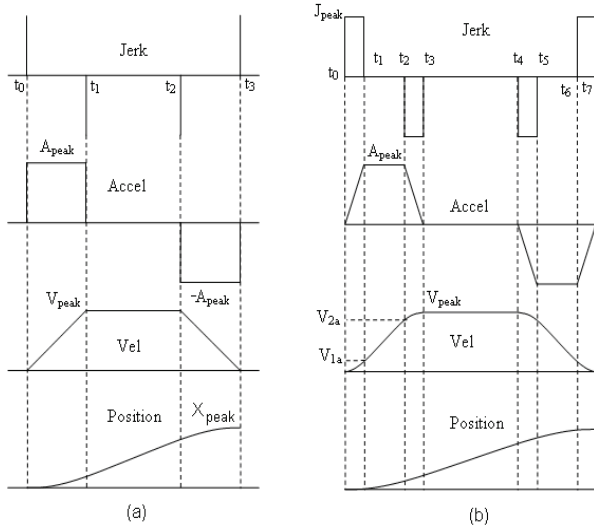


Fig. 1. Trapezoidal s-curve model (a) and third order polynomial s-curve model

2. Generalization of the polynomial s-curve model

In this paper, the highest order derivative of position profile, whose peak value is finite, is denoted the template of the model. Based on this template, the other kinematics characteristics of the motion, for example jerk, acceleration, velocity, position, etc, can be determined using its integrations.

(i) Trapezoidal velocity profile (refer to Fig.1 (a))

The following is the template of the trapezoidal model, whose velocity profile is not smooth. Its position is defined by 2nd order polynomials. So it is sometimes called 2nd order polynomial model. It is noticed that in this trapezoidal model, the jerk exhibits infinite value whenever the acceleration make a jump in value. This may be a potential problem for any system. The number of trajectory segments to be connected is 4.

$$a = \begin{cases} A_{peak}, & t_0 \leq t \leq t_1 \\ -A_{peak}, & t_2 \leq t \leq t_3 \end{cases}$$

(ii) 3rd order s-curve model (refer to Fig.1 (b))

Let the model of the trapezoidal model be M_2 , the template of the 3rd order polynomial model is defined by the below expression. For polynomial models whose orders are higher than 2, the jerks exhibit finite values. So their velocity profiles are smooth during motions. In addition their kinematic features are described by

polynomials. Therefore they are called polynomial s-curve models. The number of trajectory segments to be connected is 8.

$$j = M_3 = \begin{cases} M_2, & t_0 \leq t \leq t_3 \\ -M_2, & t_4 \leq t \leq t_7 \end{cases}$$

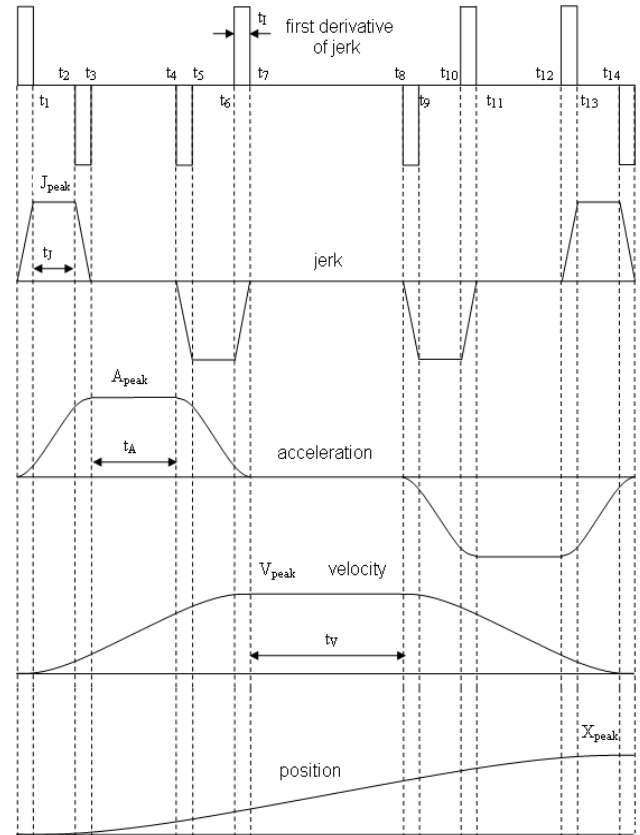


Fig. 2. Fourth order polynomial s-curve model

(iii) 4th order s-curve model (refer to Fig.2)

Similarly, the following is the template of the 4th order s-curve model. The number of trajectory segments to be connected is 16.

$$M_4 = \begin{cases} M_3, & t_0 \leq t \leq t_7 \\ -M_3, & t_8 \leq t \leq t_{15} \end{cases}$$

(iv) nth order s-curve model (refer to Fig.3)

In general, the template of the nth order s-curve model is inductively determined by the following recursive expression. The number of trajectory segments to be connected is 2^n .

$$M_n = \begin{cases} M_{n-1}, & t_0 \leq t \leq t_{2^{n-1}-1} \\ -M_{n-1}, & t_{2^{n-1}} \leq t \leq t_{2^n-1} \end{cases}$$

3. General algorithm to design s-curve motion trajectory

The conceptual method of the s-curve trajectory design is that the number of trajectory's segments is determined based on the model's template. Then the time instants of connection are calculated so that those segments are connected smoothly. So for the defined general s-curve model, the number of trajectory segments is 2^n-1 . Hence the number of time instants of connection to be calculated is 2^n .

Problem definition for the algorithm:

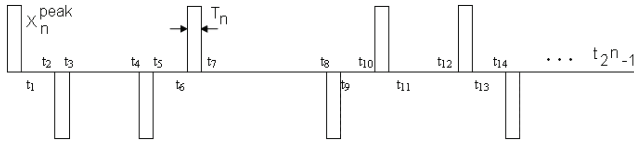


Fig.3. Template of the n^{th} order s-curve model

- Inputs: peak values of kinematic features such as $X_{0\text{peak}}, X_{1\text{peak}}, X_{2\text{peak}}, \dots, X_{n\text{peak}}$.
- Design a polynomial s-curve trajectory which is smooth, and has finite template so that no the given peak values were violated.
- Optimize the time of motion

From the definition of the general s-curve model, its kinematic features can be inductively determined as followings. It is noticed that t_k is the connection time instant of the k^{th} and $k+1^{\text{th}}$ trajectory segments, whereas T_k is the time period of the constant input $X_{k\text{peak}}$.

$$\begin{aligned} X_0^{\text{peak}} &= \frac{X_n^{\text{peak}}}{2^n} \prod_{i=1}^n (t_{2^i-1} - t_0 + T_{n+1-i}) \\ &= \frac{X_n^{\text{peak}}}{2^n} \prod_{i=1}^n \left[\left(\sum_{j=0}^{i-1} 2^j T_{n+1-i+j} \right) + T_{n+1-i} \right] \end{aligned}$$

Similarly,

$$X_1^{\text{peak}} = \frac{X_n^{\text{peak}}}{2^{n-1}} \prod_{i=1}^{n-1} \left[\left(\sum_{j=0}^{i-1} 2^j T_{n+1-i+j} \right) + T_{n+1-i} \right]$$

...

$$X_k^{\text{peak}} = \frac{X_n^{\text{peak}}}{2^{n-k}} \prod_{i=1}^{n-k} \left[\left(\sum_{j=0}^{i-1} 2^j T_{n+1-i+j} \right) + T_{n+1-i} \right]$$

...

$$X_{n-1}^{\text{peak}} = \frac{X_n^{\text{peak}}}{2} (t_1 - t_0 + T_n) = X_n T_n$$

The algorithm:

The main task of the algorithm is to calculate T_p , the time period of the constant input $X_{p\text{peak}}$. The pseudo-code of the algorithm is shown hereafter.

```

for  $p = n$  to 1  $T_p = 0$  (1)
for  $p = n$  to 1 {
     $X_0 = \frac{X_n}{2^n} \prod_{i=1}^n \left[ \left( \sum_{j=0}^{i-1} 2^j T_{n+1-i+j} \right) + T_{n+1-i} \right]$  (2)
    for  $q = 1$  to  $(p-1)$  {
         $X_q^{\text{max}} = \frac{X_n}{2^{n-q}} \prod_{i=1}^{n-q} \left[ \left( \sum_{j=0}^{i-1} 2^j T_{n+1-i+j} \right) + T_{n+1-i} \right]$  (3)
        if  $X_q^{\text{max}} > X_q^{\text{peak}}$  then
            Recalculate  $T_p$  from
             $X_q^{\text{peak}} = \frac{X_n}{2^{n-q}} \prod_{i=1}^{n-q} \left[ \left( \sum_{j=0}^{i-1} 2^j T_{n+1-i+j} \right) + T_{n+1-i} \right]$  (4)
        }
    }
}
    
```

In the algorithm, all of the time periods T_p are set to be zero by (1). T_p is first calculated by the peak value of position ($X_{0\text{peak}}$) by (2). This T_p is used to calculate the maximum value of the kinematic features X_q^{max} by (3). This maximum value is then compared with the input peak value. If the maximum value is larger than the peak value, T_p is too large. The T_p is recalculated by (4). The loop keeps going on until no peak input is exceeded.

It is noticed that (2) and (4) are polynomial equations, which have form

$$a_m x^m + a_{m-1} x^{m-1} + \dots + a_1 x^1 + a_0 = 0$$

Where a_0 is negative, and the other coefficients of the polynomial are positive. Therefore the polynomial has only one positive real root, which is just the time period to be calculated. By a simple approximating algorithm, the positive real root can be easily calculated.

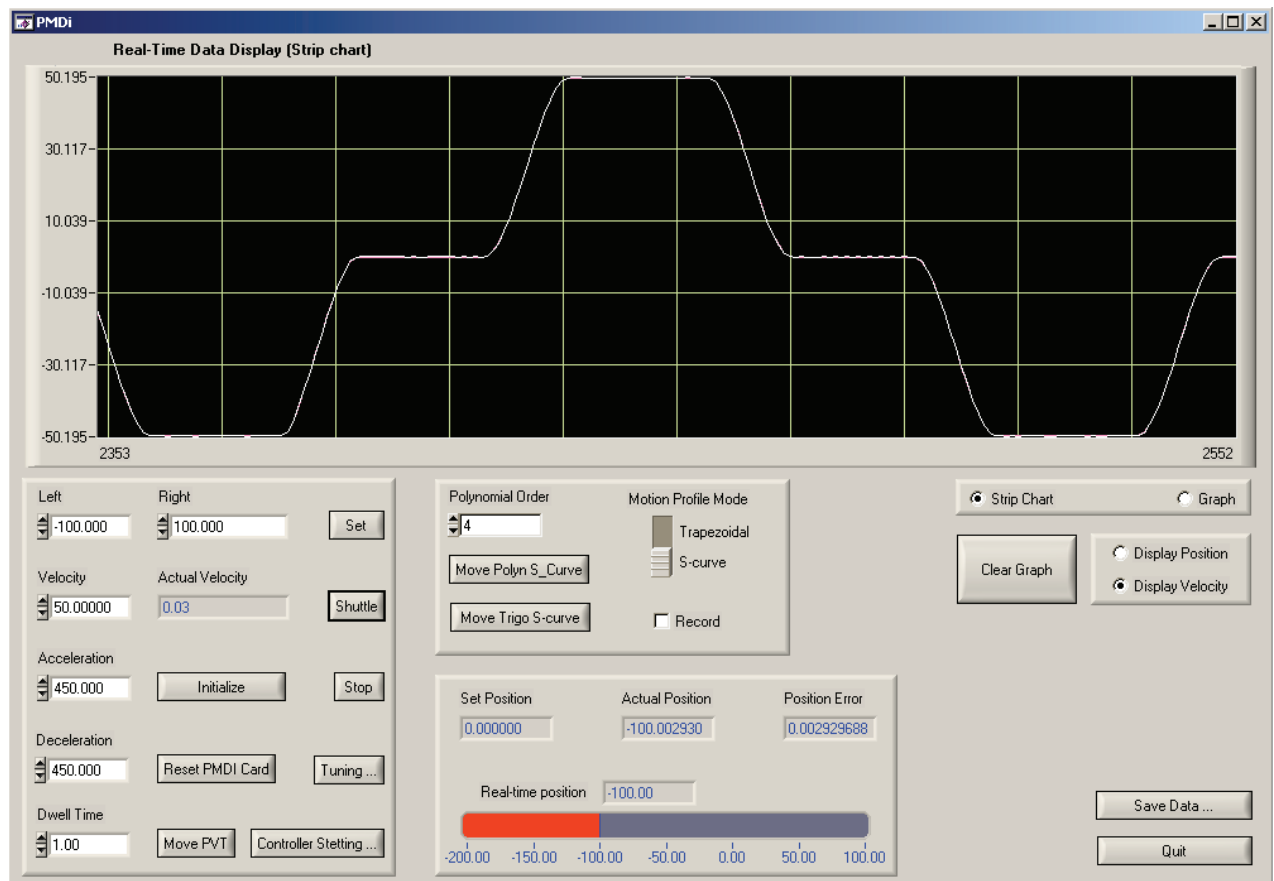


Fig. 4. PMDi Graphical User Interface

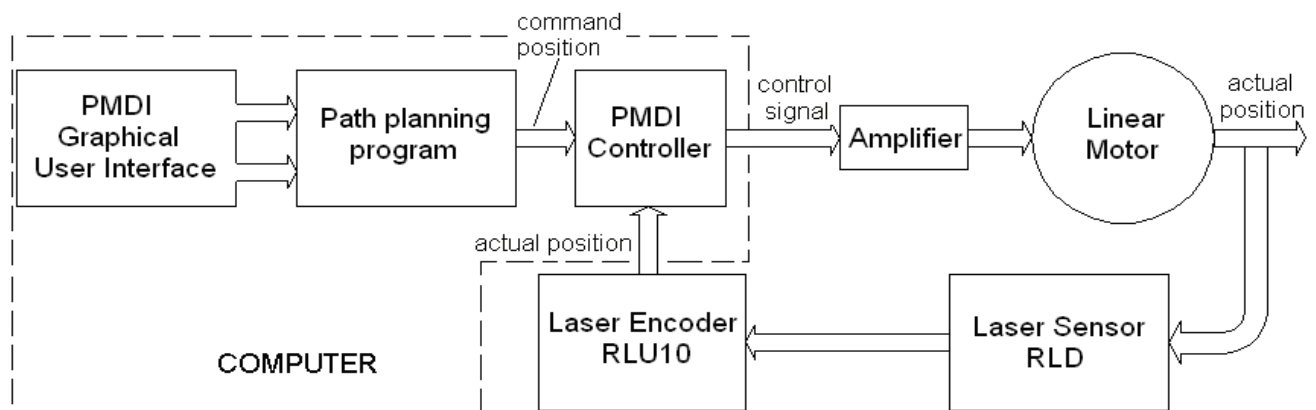


Fig. 5. Block diagram of the linear motor system

4. Experiments

4.1. Linear motor system (refer to Fig.5)

Linear motor system includes a linear motor, which slides on an air-bearing system. They allow the motor to operate smoothly and quietly with ultra-precision motion and very low friction. The linear motor is controlled by a PMDi MC4000 Pro controller card, which is an eight-axis PCI-Bus motion control DSP board provided by Precision MicroDynamics, Inc. The motor's motion is read by a laser sensor system of

Renishaw Group, including a laser sensor RLD and a laser encoder RLU10 which processes electrical signals returned by the laser sensor into quadrature signals and feeds them to the PMDi controller as feedback signals.

Users can communicate with the linear motor system through the PMDi GUI (Fig.4), which was built in C programming language with help of LabWindows/CVI development environment of National Instruments.

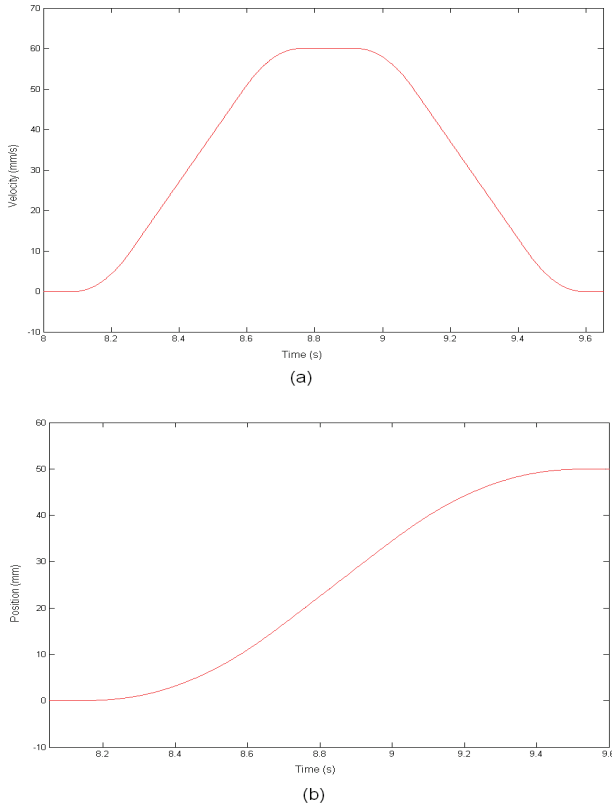


Fig. 6. Samples of velocity (a) and position (b) profiles generated using the algorithm

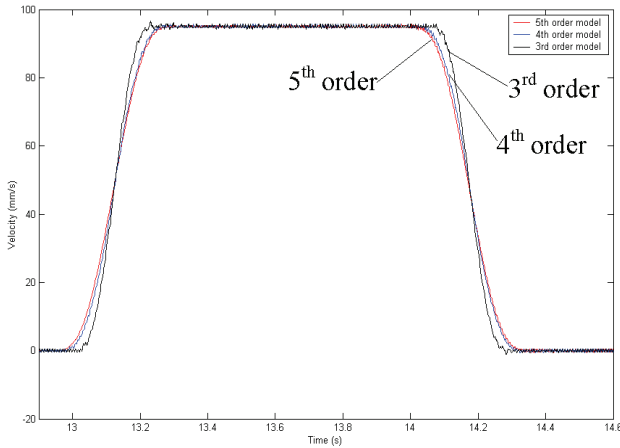


Fig. 7. Comparison of 3rd, 4th, and 5th order s-curve motion's velocity

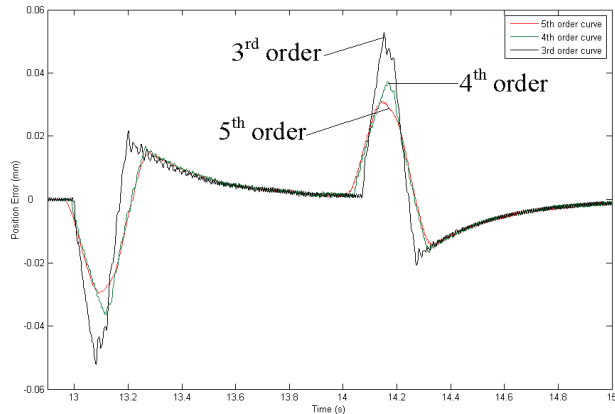


Fig. 8. Comparison of 3rd, 4th, and 5th order s-curve motion's position errors

4.2. Experimental results

The algorithm was applied to design 3rd, 4th, and 5th order polynomial s-curve profiles. The way points in form of numeric arrays, generated by the path planning program using the algorithm, were downloaded into the PMDi controller card. The controller commanded the linear motor to perform the loaded s-curve trajectories. Various experiments were carried out to study the high order polynomial s-curve motion profiles.

Fig. 6 shows the velocity profile and the trajectory planned by the algorithm. The velocity and position profiles are smooth during the motion. Additionally there is no violation of the input peak value of velocity (60mm/s) and position (50mm). A comparison of the actual velocity of the 3rd, 4th, and 5th order s-curve motions performed by the linear motor is given by Fig. 7. On the other hand, Fig. 8 illustrates the position errors of those s-curve motions. The results indicate that the higher the order of the model, the better the performance of the linear motor.

5. Trigonometric jerk model

In the attempt of looking for a new approach of developing an s-curve trajectory, a new trigonometric jerk model of s-curve was proposed, which is illuminated by the graphical representation of the model in APPENDIX B. Compared with the polynomial model illustrated in Fig.1(b), in this trigonometric model, the rectangular pulse in the jerk of the 3rd order s-curve model was replaced by a trigonometric function, which is in form of the following expressions:

Jerk,

$$j(t) = \begin{cases} \frac{J_{peak}}{2} \left[1 - \sin \left(\frac{2\pi}{t_j} t + \frac{\pi}{2} \right) \right], & 0 \leq t \leq t_1 \\ 0, & t_1 < t \leq t_2 \\ \frac{J_{peak}}{2} \left[1 - \sin \left(\frac{2\pi}{t_j} (t - t_2) + \frac{\pi}{2} \right) \right], & t_2 < t \leq t_3 \\ 0, & t_3 < t \leq t_4 \\ -\frac{J_{peak}}{2} \left[1 - \sin \left(\frac{2\pi}{t_j} (t - t_4) + \frac{\pi}{2} \right) \right], & t_4 < t \leq t_5 \\ 0, & t_5 < t \leq t_6 \\ \frac{J_{peak}}{2} \left[1 - \sin \left(\frac{2\pi}{t_j} (t - t_6) + \frac{\pi}{2} \right) \right], & t_6 < t \leq t_7 \end{cases}$$

This jerk function ensures that the whole jerk is absolutely smooth during the motor's motion, which can be referred in APPENDIX B. The trajectory is divided into 7 segments. The kinematical features can be found by the integrations of the jerk model. The APPENDIX A presents the definition of the acceleration, velocity, and position of the profile for the 7 segments.

Then many experiments were done with the linear motor system to study its performance with the motion profiles planned by the trigonometric model. Fig.9 shows the velocity and position profiles of this model, the shape is quite similar to that of the polynomial model ones. As implied in the sample results of position error in Fig.10, the response of the system with the trigonometric model perform as well as that of the 5th order polynomial model. These results can be reasonably understood by the similarity of the jerk of the two models. Both jerks are smooth, and their first derivatives exhibit sharp edges at the connection time instants. This it is concluded that though the trigonometric model is as simple as the 3rd order polynomial model, it produces as good performance as the 5th order polynomial model.

6. Conclusion

The algorithms proposed herein, which plan s-curve motion profiles with polynomial model and trigonometric model, have the ability of designing any s-curve trajectory, which is controllably smooth and time-optimal. The algorithms also ensure there is no violation of the actuator effort limitation. They can be effectively implemented by motion controllers. It is strongly believed that this works may find wide range of applications in manufacturing industry, robotics, and wherever s-curve motion appears.

However there is still plenty of room for further research on this work. We have planned to implement the algorithms to other system, for example manipulators, mobile robots, and so on, which normally require certain trajectory generator. In addition, energy consumption of the systems which use the algorithms to plan motion profiles is going to be assessed. It is reasonable to believe that the energy is optimally saved due to the smooth and jerk-bounded motions that the system perform.

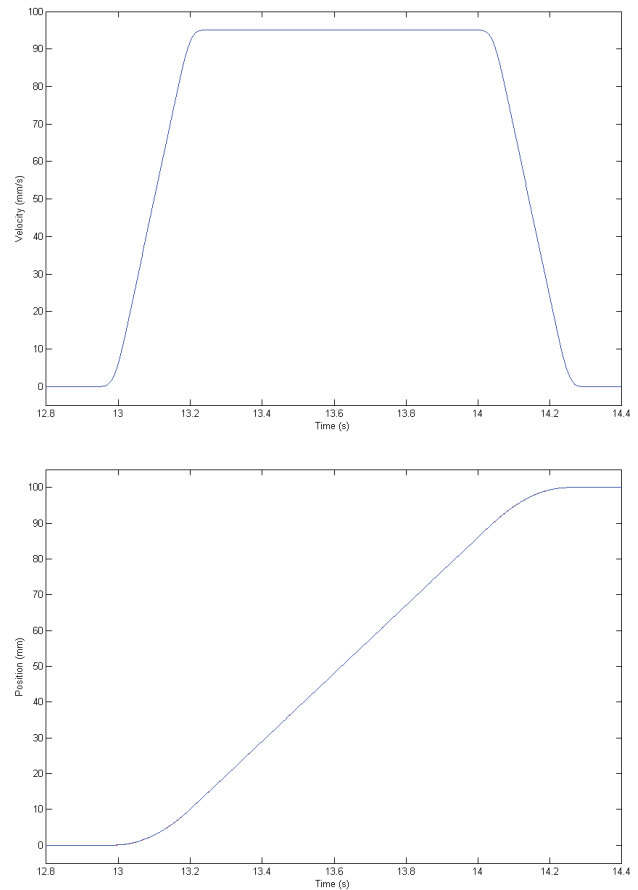


Fig. 9. Velocity and position profiles generated by the trigonometric model

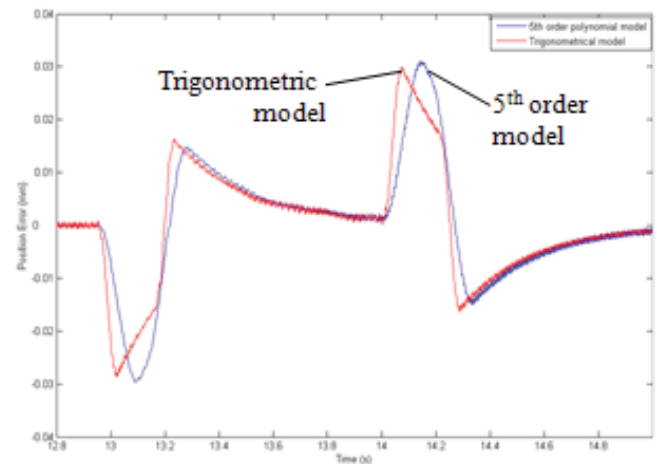


Fig. 10. Comparison of the trigonometric and 5th order models position error

7. Appendix

A. Kinematic characteristics of motion profiles planned by the trigonometric model

Acceleration,

$$a(t) = \begin{cases} \frac{J_{peak}}{2} \left[t - \left(\frac{t_J}{2\pi} \right) \cos \left(\frac{2\pi}{t_J} t + \frac{\pi}{2} \right) \right], & 0 \leq t \leq t_1 \\ A_{max}, & t_1 < t \leq t_2 \\ \frac{J_{peak}}{2} \left[(t - t_2) - \left(\frac{t_J}{2\pi} \right) \cos \left(\frac{2\pi}{t_J} (t - t_2) + \frac{\pi}{2} \right) \right] + A_{max}, & t_2 < t \leq t_3 \\ 0, & t_3 < t \leq t_4 \\ -\frac{J_{peak}}{2} \left[(t - t_4) - \left(\frac{t_J}{2\pi} \right) \cos \left(\frac{2\pi}{t_J} (t - t_4) + \frac{\pi}{2} \right) \right], & t_4 < t \leq t_5 \\ -A_{max}, & t_5 < t \leq t_6 \\ J_{peak} \left[\dots \right], & \dots \end{cases}$$

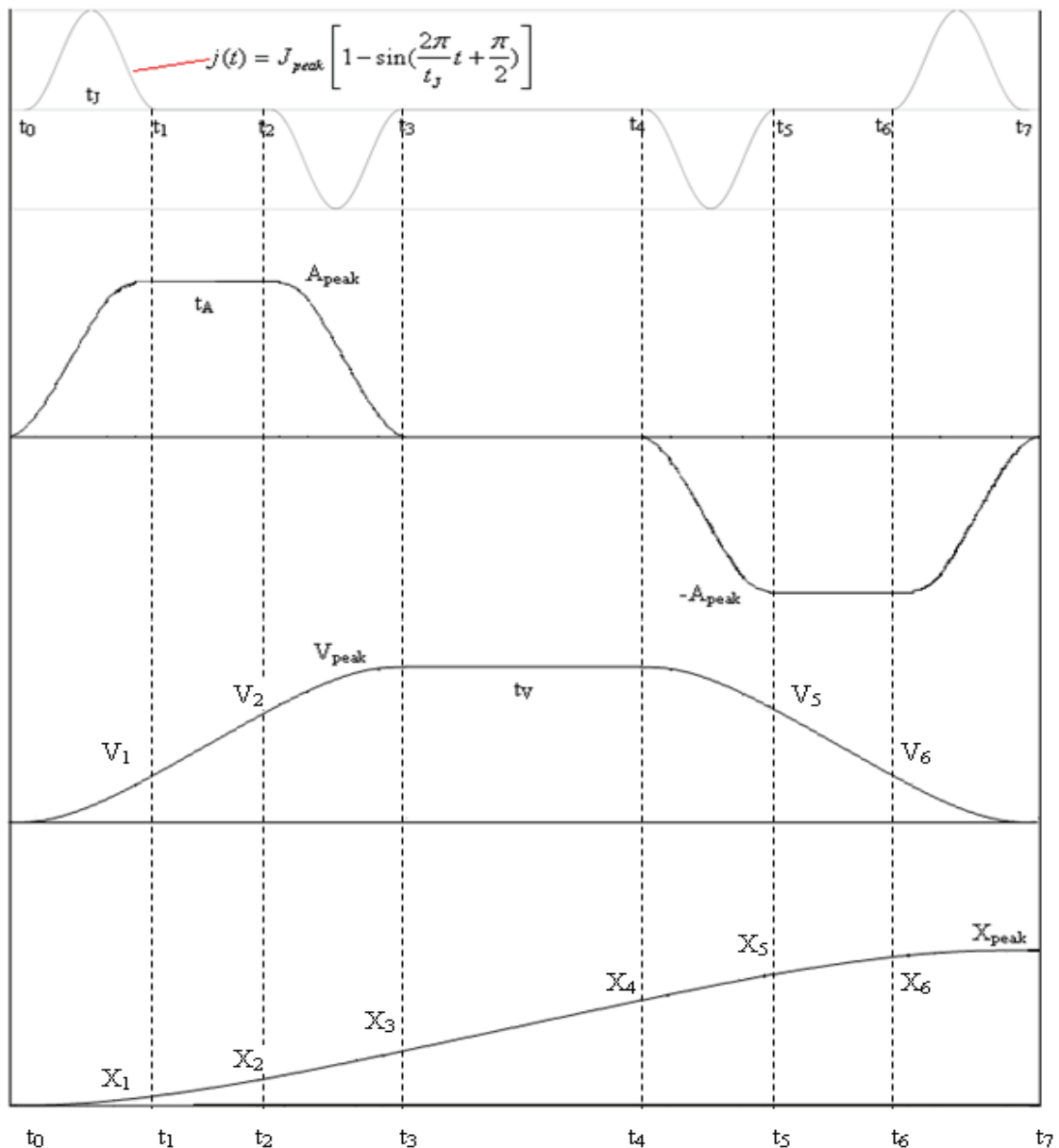
Velocity,

$$v(t) = \begin{cases} \frac{J_{peak}}{2} \left[\frac{t^2}{2} - \left(\frac{t_J}{2\pi} \right)^2 - \left(\frac{t_J}{2\pi} \right)^2 \cos \left(\frac{2\pi}{t_J} t + \frac{\pi}{2} \right) \right], & 0 \leq t \leq t_1 \\ A_{max} (t - t_1)^2 + V_1, & t_1 < t \leq t_2 \\ \frac{J_{peak}}{2} \left[\frac{(t - t_2)^2}{2} - \left(\frac{t_J}{2\pi} \right)^2 - \left(\frac{t_J}{2\pi} \right)^2 \cos \left(\frac{2\pi}{t_J} (t - t_2) + \frac{\pi}{2} \right) \right] + A_{max} (t - t_2)^2 + V_2, & t_2 < t \leq t_3 \\ V_{peak}, & t_3 < t \leq t_4 \\ -\frac{J_{peak}}{2} \left[\frac{(t - t_4)^2}{2} - \left(\frac{t_J}{2\pi} \right)^2 - \left(\frac{t_J}{2\pi} \right)^2 \cos \left(\frac{2\pi}{t_J} (t - t_4) + \frac{\pi}{2} \right) \right] + V_{max}, & t_4 < t \leq t_5 \\ -A_{max} (t - t_5)^2 + V_5, & t_5 < t \leq t_6 \\ \frac{J_{peak}}{2} \left[\frac{(t - t_6)^2}{2} - \left(\frac{t_J}{2\pi} \right)^2 - \left(\frac{t_J}{2\pi} \right)^2 \cos \left(\frac{2\pi}{t_J} (t - t_6) + \frac{\pi}{2} \right) \right] - A_{max} (t - t_6)^2 + V_6, & t_6 < t \leq t_7 \end{cases}$$

Position, $x(t) =$

$$\begin{cases} \frac{J_{peak}}{2} \left[\frac{t^3}{6} - \left(\frac{t_J}{2\pi} \right)^2 t - \left(\frac{t_J}{2\pi} \right)^3 \cos \left(\frac{2\pi}{t_J} t + \frac{\pi}{2} \right) \right], & 0 \leq t \leq t_1 \\ \frac{A_{max}}{2} (t - t_1)^2 + V_1 (t - t_1) + x(t_1), & t_1 < t \leq t_2 \\ \frac{J_{peak}}{2} \left[\frac{(t - t_2)^3}{6} - \left(\frac{t_J}{2\pi} \right)^2 (t - t_2) - \left(\frac{t_J}{2\pi} \right)^3 \cos \left(\frac{2\pi}{t_J} (t - t_2) + \frac{\pi}{2} \right) \right] + \frac{A_{max}}{2} (t - t_2)^2 + V_2 (t - t_2) + x(t_2), & t_2 < t \leq t_3 \\ V_{peak} (t - t_3) + x(t_3), & t_3 < t \leq t_4 \\ -\frac{J_{peak}}{2} \left[\frac{(t - t_4)^3}{6} - \left(\frac{t_J}{2\pi} \right)^2 (t - t_4) - \left(\frac{t_J}{2\pi} \right)^3 \cos \left(\frac{2\pi}{t_J} (t - t_4) + \frac{\pi}{2} \right) \right] + V_{max} (t - t_4) + x(t_4), & t_4 < t \leq t_5 \\ -\frac{A_{max}}{2} (t - t_5)^2 + V_2 (t - t_5) + x(t_5), & t_5 < t \leq t_6 \\ \frac{J_{peak}}{2} \left[\frac{(t - t_6)^3}{6} - \left(\frac{t_J}{2\pi} \right)^2 (t - t_6) - \left(\frac{t_J}{2\pi} \right)^3 \cos \left(\frac{2\pi}{t_J} (t - t_6) + \frac{\pi}{2} \right) \right] - \frac{A_{max}}{2} (t - t_6)^2 + V_1 (t - t_6) + x(t_6), & t_6 < t \leq t_7 \end{cases}$$

B. Graphical representation of the trigonometric model



8. References

- Kim, Y. O.; Ha, I. J. (2003), Time-optimal control of a single-DOF mechanical system considering actuator dynamics, *IEEE Transactions on Control Systems Technology*, Volume 11, Issue 6, Nov. 2003, Page(s): 919-932.
- Levin, C. (1994), Motion control gets gradually better, *Machine Design*, Nov. 7, 1994, pp. 90-94.
- Lin, F. J.; Shyu, K. K.; Lin, C. H. (2002), Incremental motion control of linear synchronous motor, *Aerospace and Electronic Systems, IEEE Transactions on*, Volume 38, Issue 3, July 2002, Page(s):1011 – 1022.
- Macfarlane, S.; Croft, E. A. (2003), Jerk-bounded manipulator trajectory planning: design for real-time applications, *IEEE Transactions on Robotics and Automation*, Volume 19, Issue 1, Feb. 2003, Page(s):42 – 52.
- Meckl, P. H. & Seering, W. P. (1985), Minimizing residual vibration for point-to-point motion, *J. of Vib., Acous., streas, and Rel. in Des.*, vol. 107, Oct. 1985, pp. 378-382.
- Meckl, P. H.; Arestides, P. B.; and Woods, M. C. (1998), Optimized s-curve motion profiles for minimum residual vibration, *Proc. Amer. Contr. Conf.*, Philadelphia, PA, June 1998, pp. 2627-2631.
- Roover, D. de (1997), *Motion Control of a Wafer Stage*, Delft University Press, The Netherlands, 1997.
- Tsay, D. M.; Lin, C. F. (2005), Asymmetrical inputs for minimizing residual response, *IEEE International Conference on Mechatronics 2005*, Taipei, Taiwan, July 2005, pp. 235- 240.